Multiscale Finite Element Formulation for the 3D Diffusion-Convection Equation

Ramoni Z. S. Azevedo[1(✉)] and Isaac P. Santos[1,2(✉)]

[1] Optimization and Computational Modeling Lab,
Federal University of Espírito Santo, Vitória, ES, Brazil
rsedano@inf.ufes.br, isaac.santos@ufes.br
[2] Department of Applied Mathematics, Federal University of Espírito Santo,
São Mateus, ES, Brazil

Abstract. In this work we present a numerical study of the Dynamic Diffusion (DD) method for solving diffusion-convection problems with dominant convection on three dimensional domains. The DD method is a two-scale nonlinear model for convection-dominated transport problems, obtained by incorporating to the multiscale formulation a nonlinear dissipative operator acting isotropically in both scales of the discretization. The standard finite element spaces are enriched with bubble functions in order to add stability properties to the numerical model. The DD method for two dimensional problems results in good solutions compared to other known methods. We analyze the impact of this methodology on three dimensional domains comparing its numerical results with those obtained using the Consistent Approximate Upwind (CAU) method.

Keywords: Dynamic diffusion method · Multiscale methods · Diffusion-convection equation

1 Introduction

The diffusive-convective transport equation plays an important role in numerous physical phenomena. It models several problems in engineering, such as the process of pollution on rivers, seas and the atmosphere; oil reservoir flow; heat transfer, and so forth [1]. However, the accurate and reliable numerical simulation of this problem is still a challenging task [2–4].

It is well known that the standard Galerkin Finite Element method (FEM) is not appropriate for solving convection-dominated problems [2], since it experiences spurious oscillations in the numerical solution, that grow as the diffusion coefficient tends to zero. The problem is caused by its loss of stability with respect to the standard H^1-norm [5]. Since the early 1980s, various stabilization techniques have been developed to overcome the weaknesses of the FEM to solve such problems.

One of the most known stabilized formulation to solve convection-dominated transport problem is the Streamline Upwind Petrov-Galerkin (SUPG) method

© Springer Nature Switzerland AG 2020
O. Gervasi et al. (Eds.): ICCSA 2020, LNCS 12251, pp. 455–469, 2020.
https://doi.org/10.1007/978-3-030-58808-3_33

(also known as the Streamline Diffusion Finite Element method (SDFEM)), proposed in [6] and analyzed in [7]. This methodology consists of adding residual-based terms to the FEM, preserving the consistency of the variational formulation. Other methodologies were developed to circumvent the difficulty of the FEM to solve problems of this nature, such as, the Galerkin-Least Square method (GLS) [8] (a variant of the SUPG), edge-based stabilization (the Continuous Interior Penalty (CIP) method [9]), and local projections (the Local Projection Stabilization (LPS) [4,10]). All these numerical formulations are capable to stabilize most of the unphysical oscillations from the FEM, caused by dominating convection. However, localized oscillations may remain in the neighborhood of sharp layers for nonregular solutions [11]. As a remedy, a number of so-called Spurious Oscillations at Layers Diminishing (SOLD) schemes have been proposed; see the excellent reviews [12,13]. SOLD schemes add additional, in general nonlinear, discontinuity (or shock-capturing) terms to these formulations in order to reduce the localized oscillations.

Residual-based stabilized methods have been reinterpreted within the context of the Variational Multiscale (VMS) framework by Hughes and collaborators in the 1990s [14–17]. The starting point of the VMS framework is the splitting of the finite element spaces into two parts: resolved (or coarse) and fine (or subgrid) subspaces. Consequently, the variational problem is decomposed into two subproblems, one associated to the resolved scales and the other associated to the fine ones. The fine scales are approximated or modeled, and then, incorporeted into the coarse scale problem, yielding in an enriched problem for the resolved scales. Many classical stabilization formulation for convection-dominated problems, such as SUPG and GLS can be reinterpreted as residual-based fine-scale models [16,18]. Also, other known multiscale methods, such as the residual-free bubbles method [19,20] and subgrid viscosity methods [21,22], can be placed within this framework.

Over the last years, some nonlinear two-scale variational methods have been developed, such as the Nonlinear Subgrid Stabilization (NSGS) [23,24] and Dynamic Diffusion (DD) methods [11,25] to solve convection-dominated problems; the Nonlinear Multiscale Viscosity (NMV) method [26,27] to solve the system of compressible Euler equations. In [28] the NSGS method was applied to solve incompressible Navier-Stokes equations. In this class of methods, bubble functions are used to enrich the standard finite element spaces and residual-based nonlinear artificial diffusion terms are added to the resulting formulation, in order to improve the stability properties of the numerical model. In particular, the DD method is obtained by incorporating to the VMS formulation, a nonlinear dissipative operator acting isotropically in both scales of the discretization. This method results in good solutions for two dimensional problems, compared to other known stabilized methods, as can be seen in [11,25].

The aim of this work is to present a numerical study of the DD method for solving steady-state diffusion-convection problems with dominant convection on three dimensional domains. We compare its computational results with the SOLD method, Consistent Approximate Upwind Petrov-Galerkin (CAU) [29], in the solution of two convection dominated problems with internal and external layers.

The remainder of this work is organized as follows. Section 2 briefly addresses the governing equation, the numerical formulations of the Galerkin finite element, CAU and DD methods. The numerical experiments are conducted in Sect. 3 and Sect. 4 concludes this paper.

2 Governing Equation and Numerical Formulation

Let $\Omega \subset \mathbb{R}^3$ be a bounded domain with a Lipschitz boundary Γ with an outward unit normal $\boldsymbol{n}$. The linear and steady-state diffusion-convection equation, with a Dirichlet boundary condition, is modeled by

$$-\kappa \Delta u + \boldsymbol{\beta} \cdot \boldsymbol{\nabla} u = f \ \text{ in } \Omega, \tag{1}$$

$$u = g \ \text{ on } \Gamma, \tag{2}$$

where u represents the quantity being transported, $\kappa > 0$ is the diffusivity coefficient, $\boldsymbol{\beta} \in [L^\infty(\Omega)]^3$ is the velocity field such that $\boldsymbol{\nabla} \cdot \boldsymbol{\beta} = 0$, $f \in L^2(\Omega)$ is a given source term and $g \in L^2(\Gamma)$ is a given function.

Consider the set of all admissible functions S and the space of test functions V defined as

$$S = \{u \in H^1(\Omega) : u = g \text{ on } \Gamma\}, \tag{3}$$

$$V = \{v \in H^1(\Omega) : v = 0 \text{ on } \Gamma\}. \tag{4}$$

The continuous variational problem associated to the boundary value problem (1) and (2) can be stated as: find $u \in S$ such that

$$A(u, v) = F(v), \quad \forall v \in V, \tag{5}$$

with

$$A(u, v) = \int_\Omega \left(\kappa \boldsymbol{\nabla} u \cdot \boldsymbol{\nabla} v + (\boldsymbol{\beta} \cdot \boldsymbol{\nabla} u) v\right) d\Omega, \tag{6}$$

$$F(v) = \int_\Omega f v \, d\Omega. \tag{7}$$

2.1 The Galerkin Finite Element Method

We consider a regular partition $\mathcal{T}_h = \{\Omega_1, \Omega_2, \ldots, \Omega_{nel}\}$ of the domain Ω into tetrahedral elements. The discrete spaces associated to S and V are defined as

$$S_h = \{u_h \in H^1(\Omega) : u_h|_{\Omega_e} \in \mathbb{P}_1(\Omega_e), \forall \Omega_e \in \mathcal{T}_h, u_h = g \in \Gamma\}, \tag{8}$$

$$V_h = \{v_h \in H^1(\Omega) : v_h|_{\Omega_e} \in \mathbb{P}_1(\Omega_e), \forall \Omega_e \in \mathcal{T}_h, v_h = 0 \in \Gamma\}, \tag{9}$$

in which $\mathbb{P}_1(\Omega_e)$ is the set of first order polynomials on local coordinates. The Galerkin formulation is obtained by restricting the problem (5) to the discrete

spaces $S_h \subset S$ and $V_h \subset V$ [2,30]. In other words, the variational statement of the approximate problem consists of finding $u_h \in S_h$, such that,

$$A_G(u_h, v_h) = F_G(v_h), \quad \forall v_h \in V_h, \tag{10}$$

where

$$A_G(u_h, v_h) = \sum_{e=1}^{nel} \int_{\Omega_e} \left(\kappa \boldsymbol{\nabla} u_h \cdot \boldsymbol{\nabla} v_h + (\boldsymbol{\beta} \cdot \boldsymbol{\nabla} u_h) v_h \right) d\Omega_e, \tag{11}$$

$$F_G(v_h) = \sum_{e=1}^{nel} \int_{\Omega_e} f v_h \, d\Omega_e. \tag{12}$$

The Galerkin finite element approximation for the variable u_h is given at the linear tetrahedral element level as follows,

$$u_h = \sum_{j=1}^{4} N_j u_j^e, \tag{13}$$

where N_j is the local interpolation function associated with the nodal point j of the element Ω_e. These functions expressed in global variables $\boldsymbol{x} = (x, y, z)$ are of the form

$$N_1 = \frac{1}{6|\Omega_e|}(a_1 + b_1 x + c_1 y + d_1 z), \qquad N_2 = \frac{1}{6|\Omega_e|}(a_2 + b_2 x + c_2 y + d_2 z),$$
$$N_3 = \frac{1}{6|\Omega_e|}(a_3 + b_3 x + c_3 y + d_3 z), \qquad N_4 = \frac{1}{6|\Omega_e|}(a_4 + b_4 x + c_4 y + d_4 z),$$

where $|\Omega_e|$ is the volume of the element, calculated by

$$|\Omega_e| = \frac{1}{6} \begin{vmatrix} 1 & x_1 & y_1 & z_1 \\ 1 & x_2 & y_2 & z_2 \\ 1 & x_3 & y_3 & z_3 \\ 1 & x_4 & y_4 & z_4 \end{vmatrix},$$

whereas the coefficients of the shape functions are given by

$$a_1 = \begin{vmatrix} x_2 & y_2 & z_2 \\ x_3 & y_3 & z_3 \\ x_4 & y_4 & z_4 \end{vmatrix}, \quad a_2 = -\begin{vmatrix} x_1 & y_1 & z_1 \\ x_3 & y_3 & z_3 \\ x_4 & y_4 & z_4 \end{vmatrix}, a_3 = \begin{vmatrix} x_1 & y_1 & z_1 \\ x_2 & y_2 & z_2 \\ x_4 & y_4 & z_4 \end{vmatrix}, \quad a_4 = -\begin{vmatrix} x_1 & y_1 & z_1 \\ x_2 & y_2 & z_2 \\ x_3 & y_3 & z_3 \end{vmatrix},$$
$$b_1 = -\begin{vmatrix} 1 & y_2 & z_2 \\ 1 & y_3 & z_3 \\ 1 & y_4 & z_4 \end{vmatrix}, \; b_2 = \begin{vmatrix} 1 & y_1 & z_1 \\ 1 & y_3 & z_3 \\ 1 & y_4 & z_4 \end{vmatrix}, \quad b_3 = -\begin{vmatrix} 1 & y_1 & z_1 \\ 1 & y_2 & z_2 \\ 1 & y_4 & z_4 \end{vmatrix}, \; b_4 = \begin{vmatrix} 1 & y_1 & z_1 \\ 1 & y_2 & z_2 \\ 1 & y_3 & z_3 \end{vmatrix},$$
$$c_1 = \begin{vmatrix} 1 & x_2 & z_2 \\ 1 & x_3 & z_3 \\ 1 & x_4 & z_4 \end{vmatrix}, \quad c_2 = -\begin{vmatrix} 1 & x_1 & z_1 \\ 1 & x_3 & z_3 \\ 1 & x_4 & z_4 \end{vmatrix}, \; c_3 = \begin{vmatrix} 1 & x_1 & z_1 \\ 1 & x_2 & z_2 \\ 1 & x_4 & z_4 \end{vmatrix}, \quad c_4 = -\begin{vmatrix} 1 & x_1 & z_1 \\ 1 & x_2 & z_2 \\ 1 & x_3 & z_3 \end{vmatrix},$$
$$d_1 = -\begin{vmatrix} 1 & x_2 & y_2 \\ 1 & x_3 & y_3 \\ 1 & x_4 & y_4 \end{vmatrix}, \; d_2 = \begin{vmatrix} 1 & x_1 & y_1 \\ 1 & x_3 & y_3 \\ 1 & x_4 & y_4 \end{vmatrix}, \quad d_3 = -\begin{vmatrix} 1 & x_1 & y_1 \\ 1 & x_2 & y_2 \\ 1 & x_4 & y_4 \end{vmatrix}, \; d_4 = \begin{vmatrix} 1 & x_1 & y_1 \\ 1 & x_2 & y_2 \\ 1 & x_3 & y_3 \end{vmatrix}.$$

The transformation from global variables $\boldsymbol{x} = (x, y, z)$ to local variables $\boldsymbol{\xi} = (\xi, \eta, \zeta)$, represented in Fig. 1, results in the following interpolation functions [31],

$$N_1 = 1 - \xi - \eta - \zeta, \quad N_2 = \xi, \quad N_3 = \eta, \quad N_4 = \zeta.$$

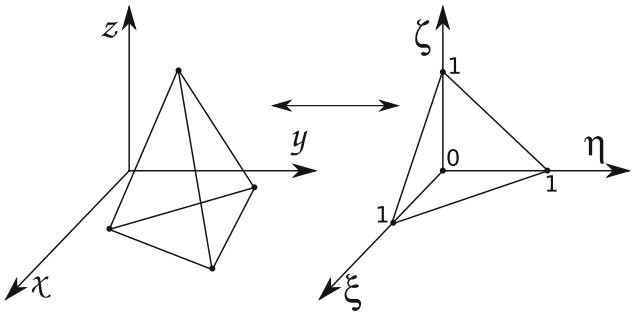

Fig. 1. Transformation from global variables (x, y, z) to local variables (ξ, η, ζ).

The matrix of transformation from global coordinates to local coordinates is defined as

$$\frac{d\boldsymbol{x}}{d\boldsymbol{\xi}} = \begin{bmatrix} \frac{\partial x}{\partial \xi} & \frac{\partial x}{\partial \eta} & \frac{\partial x}{\partial \zeta} \\ \frac{\partial y}{\partial \xi} & \frac{\partial y}{\partial \eta} & \frac{\partial y}{\partial \zeta} \\ \frac{\partial z}{\partial \xi} & \frac{\partial z}{\partial \eta} & \frac{\partial z}{\partial \zeta} \end{bmatrix} = \begin{bmatrix} x_2 - x_1 & x_3 - x_1 & x_4 - x_1 \\ y_2 - y_1 & y_3 - y_1 & y_4 - y_1 \\ z_2 - z_1 & z_3 - z_1 & z_4 - z_1 \end{bmatrix}, \tag{14}$$

and the inverse transformation matrix is determined by

$$\frac{d\boldsymbol{\xi}}{d\boldsymbol{x}} = \begin{bmatrix} \frac{\partial \xi}{\partial x} & \frac{\partial \xi}{\partial y} & \frac{\partial \xi}{\partial z} \\ \frac{\partial \eta}{\partial x} & \frac{\partial \eta}{\partial y} & \frac{\partial \eta}{\partial z} \\ \frac{\partial \zeta}{\partial x} & \frac{\partial \zeta}{\partial y} & \frac{\partial \zeta}{\partial z} \end{bmatrix} = \frac{1}{6|\Omega_e|} \begin{bmatrix} b_2 & c_2 & d_2 \\ b_3 & c_3 & d_3 \\ b_4 & c_4 & d_4 \end{bmatrix}. \tag{15}$$

The integrals present in the formulations can be easily solved analytically, using the formula for integrating products of powers of linear interpolation functions over tetrahedral elements [31],

$$\int_{\Omega_e} N_1^i N_2^j N_3^k N_4^l \, d\Omega_e = \frac{i!j!k!l!}{(i+j+k+l+3)!} 6|\Omega_e|.$$

The FEM method results in stable and accurate approximate solutions when the transport equation is diffusive dominant [6,12]. However, when the problem is convective dominant, the numerical solution may presents spurious oscillations, mainly when boundary layers (narrow regions with steep gradients) appear in the solution, requiring the use of stabilized methods [6,12,23,32]. In the following subsections we describe two different stabilization methods used to control the oscillations caused by the dominant convection.

2.2 The Consistent Approximate Upwind Method

The CAU is a stabilized method proposed in [29] for solving convection-dominated problems. It is a SOLD (discontinuity-capturing) model that consists of splitting the stabilization formulation into two parts, where the first is a linear stabilization term, the standard SUPG operator [6], and the second one is a nonlinear operator aiming to control the solution gradient, preventing localized oscillations around boundary layers. In this work we follow the CAU formulation described in [33]. The CAU formulation consists of finding $u_h \in S_h$ such that,

$$A_G(u_h, v_h) + A_{SUPG}(u_h, v_h) + A_{CAU}(u_h; u_h, v_h) = F_G(v_h) + F_{SUPG}(v_h), \quad (16)$$

$\forall v_h \in V_h$, where $A_G(u_h, v_h)$ is given by (11), and

$$A_{SUPG}(u_h, v_h) = \sum_{e=1}^{nel} \int_{\Omega_e} (-\kappa \Delta u_h + \boldsymbol{\beta} \cdot \boldsymbol{\nabla} u_h) \tau_{SUPG} (\boldsymbol{\beta} \cdot \boldsymbol{\nabla} v_h) \, d\Omega_e, \quad (17)$$

$$A_{CAU}(u_h; u_h, v_h) = \sum_{e=1}^{nel} \int_{\Omega_e} \tau_{CAU} \boldsymbol{\nabla} u_h \cdot \boldsymbol{\nabla} v_h \, d\Omega_e, \quad (18)$$

$$F_{SUPG}(v_h) = \sum_{e=1}^{nel} \int_{\Omega_e} f \tau_{SUPG} (\boldsymbol{\beta} \cdot \boldsymbol{\nabla} v_h) \, d\Omega_e. \quad (19)$$

The stabilization parameters τ_{SUPG} and τ_{CAU} are defined as follow,

$$\tau_{SUPG} = \frac{h \alpha(Pe)}{2 \|\boldsymbol{\beta}\|},$$

where $\| \cdot \|$ is the Euclidian norm in $\mathbb{R}^3$, Pe is the local Péclet number and h is the characteristic length of mesh:

$$Pe = \frac{h \|\boldsymbol{\beta}\|}{2\kappa}, \qquad \alpha(Pe) = max \left\{ 0; 1 - \frac{1}{Pe} \right\},$$

$$h = 2 \frac{\|\boldsymbol{\beta}\|}{\|\boldsymbol{\gamma}\|}, \qquad \gamma_i = \sum_{j=1}^{3} \frac{\partial \xi_i}{\partial x_j} \beta_j$$

and

$$\tau_{CAU} = \begin{cases} 0, & \text{if } \frac{|R(u_h)|}{\|\boldsymbol{\beta}\| \, \|\boldsymbol{\nabla} u_h\|} \geq \frac{\bar{\alpha}(\bar{Pe}) \bar{h}}{\alpha(Pe) h}, \\ \frac{\alpha(Pe) h}{2} \left[\frac{\bar{\alpha}(\bar{Pe}) \bar{h}}{\alpha(Pe) h} - \frac{|R(u_h)|}{\|\boldsymbol{\beta}\| \, \|\boldsymbol{\nabla} u_h\|} \right] \frac{|R(u_h)|}{\|\boldsymbol{\nabla} u_h\|}, & \text{if } \frac{|R(u_h)|}{\|\boldsymbol{\beta}\| \, \|\boldsymbol{\nabla} u_h\|} < \frac{\bar{\alpha}(\bar{Pe}) \bar{h}}{\alpha(Pe) h}, \end{cases}$$

where $R(u_h) = -\kappa \Delta u_h + \boldsymbol{\beta} \cdot \boldsymbol{\nabla} u_h - f$ is the residual of Eq. (1) on Ω_e, $\bar{Pe}$ is the local Péclet number and $\bar{h}$ the caracteristic length of mesh modifieds in termos of an auxiliary vector field $\bar{\boldsymbol{\beta}}$,

$$\bar{h} = 2 \frac{\|\boldsymbol{\beta} - \bar{\boldsymbol{\beta}}\|}{\bar{\gamma}}, \quad \bar{\gamma}_i = \sum_{j=1}^{3} \frac{\partial \xi_i}{\partial x_j} (\beta_j - \bar{\beta}_j),$$

$$\bar{Pe} = \frac{\bar{h} \|\boldsymbol{\beta} - \bar{\boldsymbol{\beta}}\|}{2\kappa}, \quad \bar{\alpha}(\bar{Pe}) = max \left\{ 0; 1 - \frac{1}{\bar{Pe}} \right\}.$$

The velocity field $\bar{\boldsymbol{\beta}}$, given by

$$\bar{\boldsymbol{\beta}} = \begin{cases} \boldsymbol{\beta}, & \text{if } \|\boldsymbol{\nabla} u_h\| = 0, \\ \boldsymbol{\beta} - \frac{|R(u_h)|}{\|\boldsymbol{\nabla} u_h\|^2} \boldsymbol{\nabla} u_h, & \text{if } \|\boldsymbol{\nabla} u_h\| > 0, \end{cases}$$

determines a new upwind direction, $\boldsymbol{\beta} - \bar{\boldsymbol{\beta}}$, calculated in each iteration in terms of the approximate solution of the previous iteration. It is important to note that the $\boldsymbol{\beta} - \bar{\boldsymbol{\beta}}$ is in the direction of $\|\boldsymbol{\nabla} u_h\|$, allowing the CAU method to possess greater stability than the SUPG method in regions near to internal and/or external boundary layers [33].

The method is solved by using an iterative procedure defined as: given u_h^n, we find u_h^{n+1} satisfying,

$$A_G(u_h^{n+1}, v_h) + A_{SUPG}(u_h^{n+1}, v_h) + A_{CAU}(u_h^n; u_h^{n+1}, v_h) = F_G(v_h) + F_{SUPG}(v_h),$$

$\forall v_h \in V_h$, where the initial solution u_h^0 is obtained by the standard Galerkin finite element method (10). The nonlinear convergence is checked under a given prescribed relative error with tolerance tol_{CAU} and a maximum number of iterations ($itmax_{CAU}$).

2.3 The Dynamic Diffusion Method

As discussed in the introduction, the DD method is a nonlinear multiscale method that consists of adding a nonlinear artificial diffusion operator acting on both scales of the discretization [11,25]. To present the DD method, we define the enriched spaces S_E and V_E, spaces of admissible functions and test functions, as

$$S_E = S_h \oplus S_B \quad \text{and} \quad V_E = V_h \oplus S_B, \tag{20}$$

where S_B is the space spanned by bubble functions. By denoting $N_b \in H_0^1(\Omega^e)$ as the bubble function defined in each element Ω_e, we define $S_B|_{\Omega_e} = span(N_b)$ and $S_B = \oplus|_{\Omega_e} S_B|_{\Omega_e}$ for all Ω_e in $\mathcal{T}_h$. Here, we use the following function [34],

$$N_b = 256 N_1(x,y,z) N_2(x,y,z) N_3(x,y,z) N_4(x,y,z),$$

where N_j is the local interpolation function associated with the nodal point j of the element Ω_e.

The discrete variational formulation of the DD method can be statement as: find $u = u_h + u_b \in S_E$, with $u_h \in S_h$ and $u_b \in S_B$, such that,

$$A_G(u, v) + A_{DD}(u_h; u, v) = F_G(v), \quad \forall v = v_h + b_b \in V_E, \tag{21}$$

with $v_h \in V_h$ and $v_b \in S_B$, where $A_G(u,v)$ and $F_G(v)$ are given by (11) and (12), respectivelly. The nonlinear operator $A_{DD}(u_h; u, v)$ in (21) is defined as

$$A_{DD}(u_h; u, v) = \sum_{e=1}^{nel} \int_{\Omega_e} \tau_{DD}(u_h) \boldsymbol{\nabla} u \cdot \boldsymbol{\nabla} v \, d\Omega_e, \tag{22}$$

where $\tau_{DD}(u_h) = \mu(h)C_b(u_h)$ represents the amount of artificial diffusion, with

$$C_b(u_h) = \begin{cases} \frac{|R(u_h)|}{2\|\boldsymbol{\nabla} u_h\|}, & \text{if} \quad \|\boldsymbol{\nabla} u_h\|\left(\frac{\|\boldsymbol{\beta}\|\mu(h)}{2\kappa} - 1\right) > 0, \\ 0, & \text{otherwise}, \end{cases} \tag{23}$$

where $R(u_h) = \boldsymbol{\beta} \cdot \boldsymbol{\nabla} u_h - f$ on Ω_e, and the caracteristic length of mesh,

$$\mu(h) = \begin{cases} 3\sqrt[3]{|\Omega_e|}, & \text{if } \Omega_e \cap \Gamma_+ \neq \emptyset, \\ \sqrt[3]{|\Omega_e|}, & \text{otherwise}, \end{cases}$$

In the last expression, $|\Omega_e|$ is the volume of the element Ω_e, $\Gamma_+ = \{\boldsymbol{x} \in \Omega_e; \boldsymbol{\beta} \cdot \boldsymbol{n} > 0\}$ is the outflow part of Γ, and $\boldsymbol{n}$ is the unit outward normal vector to the boundary Γ.

The method is solved by using an iterative procedure defined as: given u^n, we find u^{n+1} satisfying

$$A_G(u^{n+1}, v) + A_{DD}(u_h^n; u^{n+1}, v) = F_G(v), \quad \forall v \in V_E,$$

where the initial solution is $u_h^0 = 0$. To improve convergence, the following weighting rule to determine (23) is used with $w = 0.5$:

$$C_b = wC_b(u_h^{n+1}) + (1 - w)2C_b(u_h^n).$$

Using the multiscale decomposition process, the Eq. (21) results in two equations (subproblems) in each element $\Omega_e \in \mathcal{T}_h$,

$$\begin{aligned} \text{(i)} \ & \int_{\Omega_e} \kappa \boldsymbol{\nabla} u_h \cdot \boldsymbol{\nabla} v_h \, d\Omega_e + \int_{\Omega_e} (\boldsymbol{\beta} \cdot \boldsymbol{\nabla} u_h) v_h \, d\Omega_e + \int_{\Omega_e} (\boldsymbol{\beta} \cdot \boldsymbol{\nabla} u_b) v_h \, d\Omega_e \\ & + \int_{\Omega_e} \tau_{DD}(u_h) \boldsymbol{\nabla} u_h \cdot \boldsymbol{\nabla} v_h \, d\Omega_e = \int_{\Omega_e} f v_h \, d\Omega_e, \end{aligned} \tag{24}$$

$$\begin{aligned} \text{(ii)} \ & \int_{\Omega_e} (\boldsymbol{\beta} \cdot \boldsymbol{\nabla} u_h) v_b \, d\Omega_e + \int_{\Omega_e} \kappa \boldsymbol{\nabla} u_b \cdot \boldsymbol{\nabla} v_b \, d\Omega_e \\ & + \int_{\Omega_e} \tau_{DD}(u_h) \boldsymbol{\nabla} u_b \cdot \boldsymbol{\nabla} v_b \, d\Omega_e = \int_{\Omega_e} f v_b \, d\Omega_e, \end{aligned} \tag{25}$$

where we have used the known results

$$\int_{\Omega_e} (\boldsymbol{\beta} \cdot \boldsymbol{\nabla} u_b) v_b \, d\Omega_e = 0 \text{ and } \int_{\Omega_e} \boldsymbol{\nabla} u_b \cdot \boldsymbol{\nabla} v_h \, d\Omega_e = \int_{\Omega_e} \boldsymbol{\nabla} u_h \cdot \boldsymbol{\nabla} v_b \, d\Omega_e = 0,$$

since $u_h|_{\Omega_e}, v_h|_{\Omega_e} \in \mathbb{P}_1(\Omega_e)$ and $u_b, v_b \in H_0^1(\Omega_e)$.

The Eqs. (24) and (25) result in the following local system of algebraic equations, associated with each element Ω_e,

$$\begin{bmatrix} A_{hh}^e & A_{bh}^e \\ A_{hb}^e & A_{bb}^e \end{bmatrix} \begin{bmatrix} U_h^e \\ U_b^e \end{bmatrix} = \begin{bmatrix} F_h^e \\ F_b^e \end{bmatrix}, \tag{26}$$

where the local matrices and vectors in Eq. (26) are defined as follow,

$$A^e_{hh} : \int_{\Omega_e} \left(\kappa \boldsymbol{\nabla} u_h \cdot \boldsymbol{\nabla} v_h + (\boldsymbol{\beta} \cdot \boldsymbol{\nabla} u_h) v_h + \tau_{DD}(u_h) \boldsymbol{\nabla} u_h \cdot \boldsymbol{\nabla} v_h\right) d\Omega_e,$$

$$A^e_{bh} : \int_{\Omega_e} \left((\boldsymbol{\beta} \cdot \boldsymbol{\nabla} u_b) v_h\right) d\Omega_e, \quad A^e_{hb} : \int_{\Omega_e} \left((\boldsymbol{\beta} \cdot \boldsymbol{\nabla} u_h) v_b\right) d\Omega_e,$$

$$A^e_{bb} : \int_{\Omega_e} \left(\kappa \boldsymbol{\nabla} u_b \cdot \nabla v_b + \tau_{DD}(u_h) \boldsymbol{\nabla} u_b \cdot \boldsymbol{\nabla} v_b\right) d\Omega_e,$$

$$F^e_h : \int_{\Omega_e} f v_h \, d\Omega_e, \quad F^e_b : \int_{\Omega_e} f v_b \, d\Omega_e,$$

and U^e_h and U^e_b are the vectors that store the variables $u_h|_{\Omega_e}$ and u_b, respectively. Performing a static condensation to eliminate the unknowns U^e_b at each element, the system (26) can be written in terms of the macro solution U^e_h, as follows,

$$\left(A^e_{hh} - A^e_{bh}(A^e_{bb})^{-1} A^e_{hb}\right) U^e_h = F^e_h - A^e_{bh}(A^e_{bb})^{-1} F^e_b. \tag{27}$$

Remark 1. Since $\kappa > 0$, the local matrix A^e_{bb}, associated to the term

$$\int_{\Omega_e} (\kappa + \tau_{DD}(u_h)) \boldsymbol{\nabla} u_b \cdot \boldsymbol{\nabla} v_b \, d\Omega_e,$$

is always nonsingular.

The global system is obtained by assembling all local systems (27) calculated on each element Ω_e,

$$[\boldsymbol{A}_h(\boldsymbol{U}^n_h)]\boldsymbol{U}^{n+1}_h = \boldsymbol{F}_h, \tag{28}$$

$$\boldsymbol{U}^0_h = \boldsymbol{0}. \tag{29}$$

In each iteration of (28)–(29), the linear system resulting is solved by the Generalized Minimal Residual (GMRES) method [35]. The nonlinear convergence is checked under a given prescribed relative error,

$$\frac{\|\boldsymbol{U}^{n+1}_n - \boldsymbol{U}^n_h\|_\infty}{\|\boldsymbol{U}^{n+1}_n\|_\infty} \leq tol_{DD},$$

and a maximum number of iterations ($itmax_{DD}$).

3 Numerical Experiments

In this section we present two numerical experiments in order to evaluate the quality of the numerical solution obtained with the DD method in three dimensional domains. The computational code was developed in C language in a computer with the following characteristics: Intel Corel i5-2450M, CPU 2.50 GHz × 4 and 8 GB of RAM. The linear systems are solved with the GMRES method considering 150 Krylov vectors in the base, the maximum number of 100 cycles and a tolerance of 10^{-7}. For the nonlinearity of the CAU and DD methods, we use the following tolerance parameters: $tol_{CAU} = tol_{DD} = 10^{-2}$; and the following maximum number of iterations: $itermax_{CAU} = itermaxDD = 50$.

3.1 Problem 1

This problem simulates a three dimensional convection-dominated diffusion-convection problem, with internal and external layers, in a unit cube $\Omega =]0,1[^3$ with the following coefficients: $\kappa = 10^{-9}$, $\boldsymbol{\beta} = (0,1,0)^T$ and $f = 1$. The Dirichlet boundary conditions are defined as $u = 0$ on all faces except in the plane $y = 0$, where a jump discontinuity is introduced in the inflow boundary,

$$u(x,0,z) = \begin{cases} 1, & \text{for } 0 \leq x \leq 0.5, \quad z \in [0,1], \\ 0, & \text{for } 0.5 < x \leq 1, \quad z \in [0,1]. \end{cases}$$

The domain Ω was partitioned in 32 divisions in each direction, so the mesh has 35937 nodes and 196608 elements.

Due to the difficulty in representing results in 3D domains, the solutions are exhibited at the xy plane located at $z = 0.5$. Figure 2 shows the solutions obtained by the CAU and DD methods. The CAU solution (Fig. 2(a)) appears more diffusive in the external boundary layers (narrow regions close to Γ where $\|\boldsymbol{\nabla} u\|$ is large) at $x = 0$, $x = 1$ and $y = 1$, whereas the DD method (Fig. 2(b)) presents some nonphysical under/overshoots in the external layer, at $y = 1$, mainly for $x > 0.5$. In the internal layer, both methods present some diffusion in the region next to the outflow boundary.

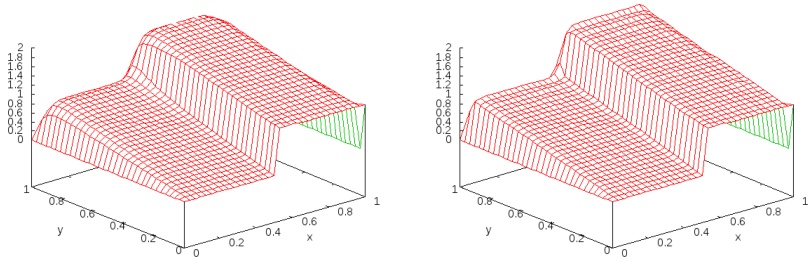

(a) CAU solution (b) DD solution

Fig. 2. Solutions in plane $z = 0.5$.

For a better understanding of the behavior of the CAU and DD methods, we made three cuts (cross sections) in the solutions described in Fig. 2, at $x = 0.25$, $x = 0.75$ and $y = 0.9$. Figure 3(a) shows the cross section at $x = 0.25$ (lower graph) and at $x = 0.75$ (upper graph). We can observe the diffusive behavior of the CAU method in the external boundary layer (at $y = 1$). In this region the DD solution is better, despite the slight under/overshoots. Figure 3(b) shows the cross section at $y = 0.9$. The CAU method is more diffusive in the three layers at $x = 0$, $x = 0.5$ and $x = 1$.

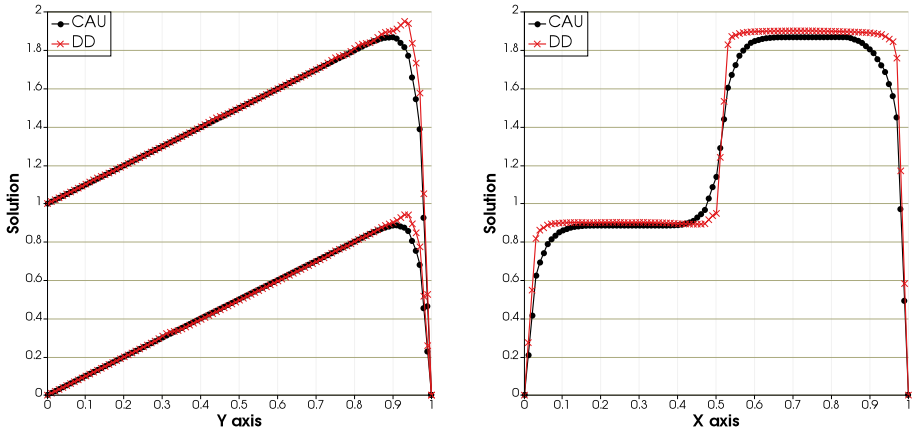

(a) (b)

Fig. 3. (a) Solutions at $z = 0.5$ and $x = 0.25$ (top), $x = 0.75$ (bottom). (b) Solutions at $z = 0.5$ and $y = 0.9$.

3.2 Problem 2

In this experiment we consider a convection-dominated diffusion-convection problem defined on $\Omega =]0,1[^3$ with the following coefficients: $\kappa = 10^{-6}$, $\boldsymbol{\beta}(1,1,1)^T$ and $f = 1$. The Dirichlet boundary conditions are defined as $u = 0$ on faces $x = 0$, $y = 0$ and $z = 0$ and $u = 1$ on faces $x = 1$, $y = 1$ and $z = 1$. The mesh used in this experiment is the same one as the Problem 1.

The solutions are exposed at the xy plane located at $z = 0.5$. Figure 4 shows the solutions obtained by the CAU and DD methods. The solution obtained with the CAU method appears to be more diffusive at the external boundary layer at $x = 1$ and at $y = 1$ than that of Fig. 4(b). However, some non physical under/overshoots localized at the external layer remain in the DD solution.

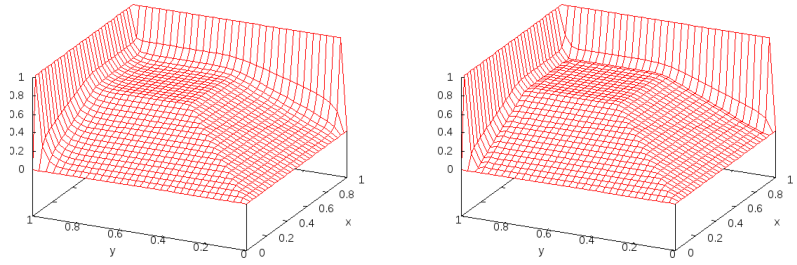

(a) CAU solution (b) DD solution

Fig. 4. Solutions in plane $z = 0.5$.

These numerical solutions are better understood, analyzing the cuts (cross section) of them shown in the Fig. 5, Fig. 5(a) shows the cross section at $x = 0.7$ and Fig. 5(b) shows the cross section at $y = 0.9$, and Fig. 6 shows the cross section along the diagonal of the xy plane. All of them show the more diffusive behavior of the CAU method in the boundary layer regions and the small oscillations presented by the DD method solution.

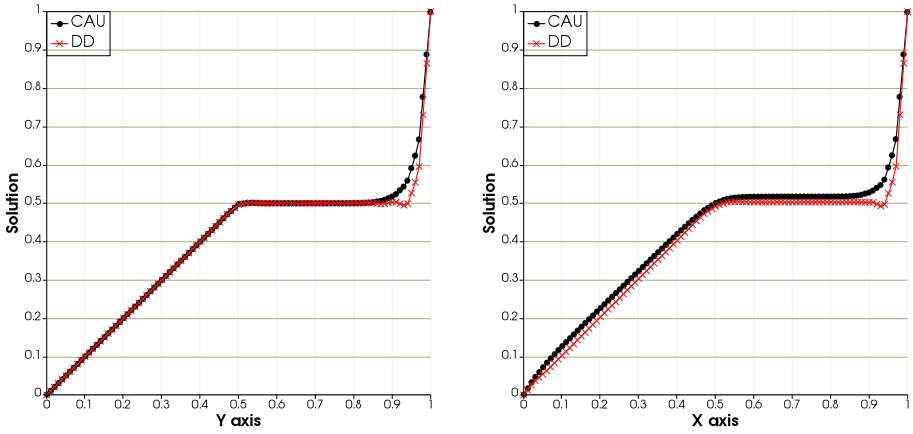

(a) (b)

Fig. 5. (a) Solutions at $z = 0.5$ and $x = 0.7$. (b) Solutions at $z = 0.5$ and $y = 0.9$.

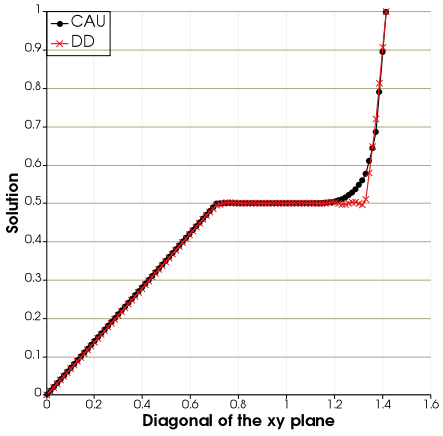

Fig. 6. Solutions along the diagonal of the xy plane at $z = 0.5$.

4 Conclusions

This work deals with the evaluation of the DD method in the solution of diffusion-convection problems with dominant convection on three dimensional domains. We studied two problems with internal and external layers, comparing the results obtained with those from the CAU method. In both experiments, the DD method obtained solutions less diffusive than the CAU, but with small under/overshoot in the external layers.

As in two dimensional problems, the DD method proved to be a promising methodology for solving convection-dominated problems on three dimensional domains. However, more numerical experiments need to be carried out in order to strengthen our conclusions. As future work, we plan to apply this methodology for solving 3D unsteady transport problems, including the Navier-Stokes equations, and also to investigate the convergence rates for the errors in norms $L^2(\Omega)$ and $H^1(\Omega)$.

Acknowledgments. The authors would like to thank the support through the Espírito Santo State Research Support Foundations (FAPES), under Grant Term 181/2017, and the Coordenação de Aperfeiçoamento de Pessoal de Nível Superior - Brasil (CAPES) - Finance Code 001.

References

1. Dehghan, M.: On the numerical solution of the one-dimensional convection-diffusion equation. Math. Probl. Eng. **2005**(1), 61–74 (2005)
2. Donea, J., Huerta, A.: Finite Element Method for Flow Problems. Wiley, Hoboken (2003)
3. Bause, M.: Stabilized finite element methods with shock-capturing for nonlinear convection-diffusion-reaction models. In: Kreiss, G., Lötstedt, P., Målqvist, A., Neytcheva, M. (eds.) ENUMATH 2009, Numerical Mathematics and Advanced Applications 2009, pp. 125–133. Springer, Heidelberg (2010). https://doi.org/10.1007/978-3-642-11795-4_12
4. Barrenechea, G.R., John, V., Knobloch, P.: A local projection stabilization finite element method with nonlinear crosswind diffusion for convection-diffusion-reaction equations. ESAIM: Math. Model. Numer. Anal. **47**(5), 1335–1366 (2013)
5. Roos, H., Stynes, M., Tobiska, L.: Robust Numerical Methods for Singularly Perturbed Differential Equations: Convection-Diffusion-Reaction and Flow Problems, 2nd edn. Springer Science & Business Media, Berlin (2008). https://doi.org/10.1007/978-3-540-34467-4
6. Brooks, A.N., Hughes, T.J.R.: Streamline upwind Petrov-Galerkin formulations for convection dominated flows with particular emphasis on the incompressible Navier-Stokes equations. Comput. Methods Appl. Mech. Eng. **32**(1–3), 199–259 (1982)
7. Johnson, C., Nävert, U., Pitkäranta, J.: Finite element methods for linear hyperbolic problems. Comput. Methods Appl. Mech. Eng. **45**(1), 285–312 (1984)
8. Hughes, T.J.R., Franca, L.P., Hulbert, G.M.: A new finite element formulation for computational fluid dynamics: VIII. the Galerkin/Least-Squares method for advective-diffusive equations. Comput. Methods Appl. Mech. Eng. **73**(2), 173–189 (1989)

9. Burman, E., Hansbo, P.: Edge stabilization for Galerkin approximations of convection-diffusion-reaction problems. Comput. Methods Appl. Mech. Eng. **193**(15), 1437–1453 (2004)
10. Barrenechea, G.R., Burman, E., Karakatsani, F.: Blending low-order stabilised finite element methods: a positivity-preserving local projection method for the convection-diffusion equation. Comput. Methods Appl. Mech. Eng. **317**, 1169–1193 (2017)
11. Valli, A.M.P., Almeida, R.C., Santos, I.P., Catabriga, L., Malta, S.M.C., Coutinho, A.L.G.A.: A parameter-free dynamic diffusion method for advection-diffusion-reaction problems. Comput. Math. Appl. **75**(1), 307–321 (2018)
12. John, V., Knobloch, P.: On spurious oscillations at layers diminishing (SOLD) methods for convection-diffusion equations: part I - a review. Comput. Methods Appl. Mech. Eng. **196**(17), 2197–2215 (2007)
13. John, V., Knobloch, P.: On spurious oscillations at layers diminishing (SOLD) methods for convection-diffusion equations: part II - analysis for P1 and Q1 finite elements. Comput. Methods Appl. Mech. Eng. **197**(21–24), 1997–2014 (2008)
14. Hughes, T.J.R.: Multiscale phenomena: Green's functions, the Dirichlet-to-Neumann formulation, subgrid scale models, bubbles and the origins of stabilized methods. Comput. Methods Appl. Mech. Eng. **127**(1–4), 387–401 (1995)
15. Hughes, T.J.R., Stewart, J.R.: A space-time formulation for multiscale phenomena. J. Comput. Appl. Math. **74**(1–2), 217–229 (1996)
16. Brezzi, F., Franca, L.P., Hughes, T.J.R., Russo, A.: b = ∫g. Comput. Methods Appl. Mech. Eng. **145**, 329–339 (1997)
17. Hughes, T.J.R., Feijóo, G.R., Mazzei, L., Quincy, J.-B.: The variational multiscale method - a paradigm for computational mechanics. Comput. Methods Appl. Mech. Eng. **166**(1–2), 3–24 (1998)
18. Hughes, T.J.R., Scovazzi, G., Franca, L.P.: Multiscale and stabilized methods. In: Encyclopedia of Computational Mechanics, 2nd edn, pp. 1–64 (2018)
19. Brezzi, F., Russo, A.: Choosing bubbles for advection-diffusion problems. Math. Models Methods Appl. Sci. **4**(4), 571–587 (1994)
20. Franca, L.P., Nesliturk, A., Stynes, M.: On the stability of residual-free bubbles for convection-diffusion problems and their approximation by a two-level finite element method. Comput. Methods Appl. Mech. Eng. **166**(1–2), 35–49 (1998)
21. Guermond, J.-L.: Stabilization of Galerkin approximations of transport equation by subgrid modeling. Math. Model. Numer. Anal. **33**, 1293–1316 (1999)
22. Guermond, J.-L.: Subgrid stabilization of Galerkin approximations of linear monotone operators. IMA J. Numer. Anal. **21**, 165–197 (2001)
23. Santos, I.P., Almeida, R.C.: A nonlinear subgrid method for advection-diffusion problems. Comput. Methods Appl. Mech. Eng. **196**(45–48), 4771–4778 (2007)
24. Santos, I.P., Almeida, R.C., Malta, S.M.C.: Numerical analysis of the nonlinear subgrid scale method. Comput. Appl. Math. **31**(3), 473–503 (2012)
25. Arruda, N. C. B., Almeida, R. C., Dutra do Carmo, E. G.: Dynamic diffusion formulations for advection dominated transport problems. In: Dvorkin, E., Goldschmit, M., Storti, M. (eds.) Mecánica Computacional. vol. 29, pp. 2011–2025. Asociación Argentina de Mecánica Computacional, Buenos Aires (2010)
26. Bento, S.S., de Lima, L.M., Sedano, R.Z., Catabriga, L., Santos, I.P.: A nonlinear multiscale viscosity method to solve compressible flow problems. In: Gervasi, O., et al. (eds.) ICCSA 2016. LNCS, vol. 9786, pp. 3–17. Springer, Cham (2016). https://doi.org/10.1007/978-3-319-42085-1_1

27. Bento, S. S., Sedano, R. Z., Lima, L. M., Catabriga, L., Santos, I. P.: Comparative studies to solve compressible problems by multiscale finite element methods. Proc. Ser. Braz. Soc. Comput. Appl. Math. **5**(1) (2017). https://doi.org/10.5540/03.2017.005.01.0317
28. Baptista, R., Bento, S.S., Santos, I.P., Lima, L.M., Valli, A.M.P., Catabriga, L.: A multiscale finite element formulation for the incompressible Navier-Stokes equations. In: Gervasi, O., et al. (eds.) ICCSA 2018. LNCS, vol. 10961, pp. 253–267. Springer, Cham (2018). https://doi.org/10.1007/978-3-319-95165-2_18
29. Galeão, A.C., Dutra do Carmo, E.G.: A consistent approximate upwind Petrov-Galerkin method for convection-dominated problems. Comput. Methods Appl. Mech. Eng. **68**(1), 83–95 (1988)
30. Raviart, P.A., Thomas, J.M.: Introduction à l'analyse numérique des équations aux dérivées partielles. Masson, Paris (1992)
31. Hughes, T. J. R.: The Finite Element Method: Linear Static and Dymanic Finite Element Analysis. Prentice-Hall International (1987)
32. Galeão, A.C., Almeida, R.C., Malta, S.M.C., Loula, A.F.D.: Finite element analysis of convection dominated reaction-diffusion problems. Appl. Numer. Math. **48**(2), 205–222 (2004)
33. Carmo, E.G.D., Alvarez, G.B.: A new stabilized finite element formulation for scalar convection-diffusion problems: the streamline and approximate upwind/Petrov-Galerkin method. Comput. Methods Appl. Mech. Eng. **192**(31–32), 3379–3396 (2003)
34. Ern, A., Guermond, J.-L.: Theory and Practice of Finite Elements, vol. 159, 1st edn. Springer Science & Business Media, New York (2004). https://doi.org/10.1007/978-1-4757-4355-5
35. Saad, Y., Schultz, H.: GMRES: a generalized minimal residual algorithm for solving nonsymmetric linear systems. SIAM. J. Sci. Stat. Comput. **7**(3), 856–869 (1986)